1 August 2000

OPTICS COMMUNICATIONS

ELSEVIER

Optics Communications 182 (2000) 205–208

www.elsevier.com/locate/optcom

Efficient formation of pure helical laser beams

Ram Oron [a,*], Nir Davidson [a], Asher A. Friesem [a], Erez Hasman [b]

[a] *Weizmann Institute of Science, Department of Physics of Complex Systems, Rehovot 76100, Israel*
[b] *Technion - Israel Institute of Technology, Optical Engineering Group, Faculty of Mechanical Engineering, Haifa 32000, Israel*

Received 17 February 2000; received in revised form 1 June 2000; accepted 5 June 2000

Abstract

A novel method for forming pure helical laser beams of pre-determined helicity is presented. It is mainly based on replacing one of the laser mirrors with a spiral phase element. The basic principles along with experimental results using a CO_2 laser are described. © 2000 Elsevier Science B.V. All rights reserved.

PACS: 41.85.Ct; 41.85.Ew; 42.60.Jf; 42.60.Da
Keywords: Laser beams; Phase elements

1. Introduction

Recent years have witnessed a growing interest in helical laser beams [1–14]. Such beams have the shape of a continuous helical (or spiral) phase, and can be exploited in a variety of applications. These include optical transformations [1], frequency shifting [2], angular momentum transfer [3], trapping of microscopic particles [4] and atoms [5], the study of optical vortices [6] and specialized alignment schemes [7].

Typically, helical laser beams are formed by manipulating the light after it emerges from a laser. For example, by superposition of two orthogonal (non-helical) beams [8] or by transforming Gaussian beams into helical beams [9–11]. The superposition is achieved by means of beam splitters and mirrors [8], whereas the transformation by means of computer generated holograms [9], cylindrical lenses [10] and spiral phase plates [11]. Such helical beam formations are generally either cumbersome or lead to an undesirable combination of helical beams. Moreover, the conversion efficiency is relatively low.

Alternatively it is possible to form helical modes inside the laser resonator, so as to directly obtain a helical beam emerging from the laser. Specifically, combinations of helical Laguerre–Gaussian modes were formed by inserting a Dove prism into a ring-laser [12], but these do not form a pure single mode. Unstable resonators with helical mirrors were analysed theoretically [13]. Also, helical modes were formed by a superposition of two orthogonal (non-helical) modes [14], but this method required sophisticated alignment procedures of intra-cavity absorber and apertures for controlling the transverse modes, as well as modifying the astigmatism of the resonator in order to mode-lock the two orthogonal modes. Also,

* Corresponding author. Fax: +972 8 9344109; e-mail: ram.oron@weizmann.ac.il

PII: S0030-4018(00)00804-X

there is no definite procedure to control the helicity of the emerging helical beam.

In a related effort, spiral phase elements (SPEs) were inserted into laser resonators in order to discriminate and select a single high order Laguerre–Gaussian mode having a helical phase distribution inside the laser resonator [15]. Yet, the beam emerging from the laser had an annular intensity distribution with uniform phase, so the far field intensity distribution was nearly Gaussian. In this paper, we exploit a similar mode selection method with a new laser resonator configuration, so that the beam emerging from the laser has a helical phase distribution both in the near and far fields. Specifically, we demonstrate, for the first time, that it is possible to obtain single frequency pure and stable helical beams with pre-determined helicity, from a laser resonator. Moreover, we show both theoretically and experimentally, how to distinguish between helical and doughnut beams, and between helical beams of opposite helicity. In the following we present the principles of our approach and the design of the SPEs, along with representative experimental results with a CO_2 laser.

2. Basic principles

The formation of pure helical laser modes is achieved by inserting into the laser resonator SPEs that are essentially lossless for the desired helical mode, but introduce high losses to all other modes. The laser resonator configuration for forming a helical beam is shown in Fig. 1. Here, the back mirror is replaced with a reflective SPE, which changes the phase of the wavefront upon reflection by

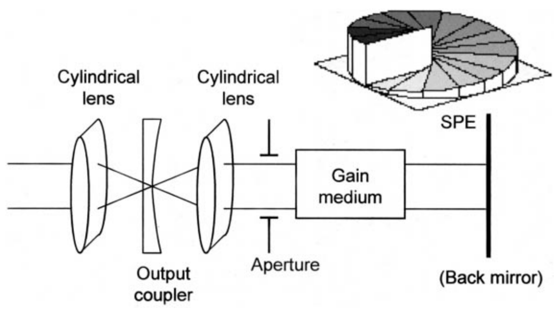

Fig. 1. Laser resonator configuration for forming a helical beam.

$\exp(+2il\theta)$ where l is the desired helical mode order. Thus, a helical mode with phase of $\exp(-il\theta)$ is converted into $\exp(+il\theta)$ after reflection by the SPE. The cylindrical lens, which is located inside the resonator and focused on the output coupler, inverts the helicity of the mode back to $\exp(-il\theta)$ after a round trip, to ensure self consistency of the desired helical mode. The beam emerging from the resonator passes through another external cylindrical lens, so its distribution will have the same form as the intracavity helical mode pattern. The aperture inside the resonator ensures that the laser operate with the lowest order helical mode, i.e. TEM_{0l^*}.

The resulting field distribution $E(r,\theta)$ for the TEM_{0l^*} mode is

$$E(r,\theta) = E_0\,\varrho^{l/2}L_0^l(\varrho)\exp(-\varrho/2)\exp(-il\theta), \tag{1}$$

where r and θ are the cylindrical coordinates, E_0 the magnitude of the field, $\varrho = 2r^2/w^2$ with w as the spot size of the Gaussian beam, and L_0^l are the generalized Laguerre polynomials of order 0 and index l. For $l=1$ we obtain the lowest order helical mode of $E(r,\theta) = E_0\sqrt{\varrho}\exp(-\varrho/2)\exp(-i\theta)$. It is important to note that the helicity of the SPE determines the helicity of the helical mode in the laser resonator. Consequently, by designing the SPE with specific helicity, it is possible to control the helicity of the helical beam emerging from the laser.

In general the intensity distribution of a helical laser beam has the same distribution, as that of doughnut-shaped laser beam, but their field distribution are distinctly different. Specifically, the doughnut-like laser beams are composed of an incoherent superposition of two orthogonal Cartesian modes $TEM_{0l(x)}$ and $TEM_{0l(y)}$, where the field distributions are

$$E_x(r,\theta) = E_0\,\varrho^{l/2}L_0^l(\varrho)\exp(-\varrho/2)\cos(l\theta);$$

$$E_y(r,\theta) = E_0\,\varrho^{l/2}L_0^l(\varrho)\exp(-\varrho/2)\sin(l\theta) \tag{2}$$

When the two field distributions $E_x(r,\theta)$ and $E_y(r,\theta)$, in Eq. (2), are added incoherently they form a hybrid mode whose intensity distribution has a doughnut shape. On the other hand, when they are added coherently with the appropriate phase, they form a pure helical mode. In order to distinguish between the hybrid and the helical modes it is best to let the emerging beam pass through another SPE. An SPE having a phase of $\exp(+il\theta)$ will focus the helical beam to obtain a high central peak, whereas one having a phase of $\exp(-il\theta)$ will diverge it further away from the center. This property is unique to the helical TEM_{0l^*} modes. For the beams formed by the hybrid mode, either one of these two SPEs will focus the hybrid beam to a high central peak, since either of the SPEs cause all parts of the modes to be approximately in phase.

3. Experimental procedure and results

Our method was experimentally verified with a linearly polarized discharge pumped CO_2 laser, operating with a single longitudinal mode, in a configuration shown in Fig. 1. The reflective SPE was fabricated on a silicon substrate in a multi-stage etching process, to form 32 phase levels with a combined depth of λ, which corresponds to $l=1$.

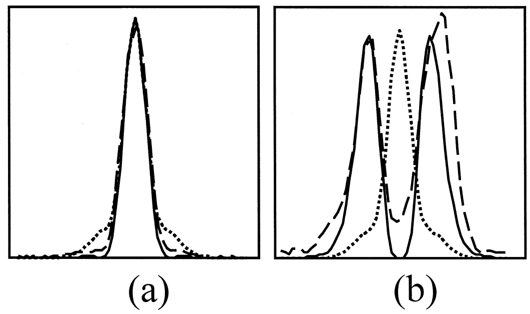

Fig. 3. Far field intensity distribution cross sections (dashed lines) with an additional transmittive SPE which introduces an additional phase of (a) $\exp(-il\theta)$ (b) $\exp(+il\theta)$, along with theoretical results for the coherent – helical (solid lines) and incoherent – hybrid (dotted lines) cases. Scale is similar to Fig. 2(d).

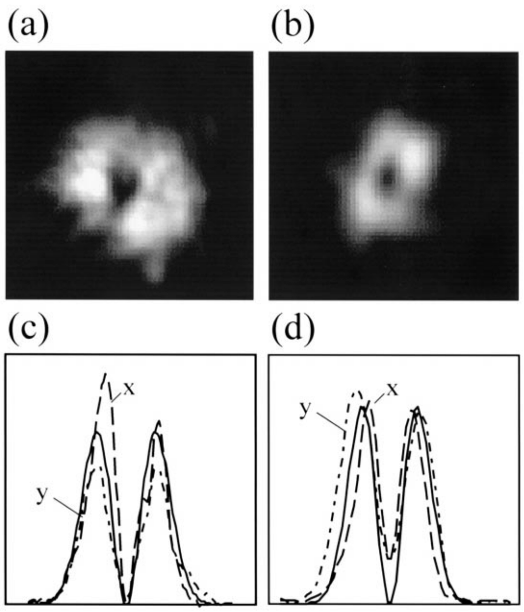

Fig. 2. Near- and far-fields intensity distributions of a helical beam. (a) Experimental near-field intensity distribution. (b) Experimental far-field intensity distribution. (c) Predicted and experimental near-field intensity distribution cross sections; experimental results for the x and y axes are shown in dashed lines whereas predicted results are represented by solid lines. (d) Predicted and experimental far-field intensity distribution cross sections.

The depth accuracy in the fabrication process was less than 3% and the RMS surface quality was better than 20 nm. Its reflectivity was better than 98%, adequate to serve as a laser reflector mirror. The diameter of the laser tube was 11 mm, and the length of the laser was 65 cm. The intra-cavity cylindrical lens ($f = 12.5$ cm) was focused on the concave ($r = 3$ m) output coupler, whereas an identical lens was positioned outside the cavity to collimate the output beam.

Some representative experimental results are shown in Figs. 2 and 3. Fig. 2 shows the near- and far-field intensity distributions of a helical beam that emerges from the laser (after passing through the external cylindrical lens). The near-field distribution, shown in Fig. 2(a), has the expected doughnut shape, albeit with some distortions, caused mainly by imperfections in the fabrication process of the SPE. The output power was 1.2 W. The corresponding far-field intensity distribution, shown in Fig. 2(b) was obtained by focusing the output beam with a spherical lens ($f = 50$ cm). Here we see again the doughnut shape. The x and y cross sections of the near- and far-field intensity distributions, compared to the expected cross sections, derived from Eq. (1), are given in Fig. 2(c) and Fig. 2(d) respectively. As evident, there is good agreement between the predicted and experimental results, including the low intensity at the center. As shown, there was some asymmetry between the x and y cross sections of the intensity distributions. We believe that is due to some astigmatism caused by the intra-cavity cylindrical lens. We also measured the intensity distribution at other planes around the focal plane. In these the doughnut-shaped distributions are still clearly evident with low intensity at the center, albeit with slightly growing diameter further away from the focal plane. These results indicate that the beam maintains its shape as it propagates along the z-axis.

To ensure that a pure helical beam, having a phase of $\exp(-i\theta)$, was formed, it is possible to examine the interference of the beam with its mirror image or with a reference beam [14]. We exploited an alternative method, where we let the emerging beam pass through one of two SPEs before measuring the far field intensity distribution. The first SPE with a phase of $\exp(+i\theta)$ was designed to correct the phase of the near field pattern so it will be uniform, whereas the second SPE with a phase of $\exp(-i\theta)$ was designed to add another spiral like phase. The measured results are shown in Fig. 3, along with these predicted for hybrid and helical beams. Fig. 3(a) shows the cross sections of the far-field intensity distributions with the first phase correcting SPE. As evident, there is a high central peak, and very low side lobes, in agreement with those predicted for a helical beam, whilst the incoherent hybrid beam has more power spreading. Fig. 3(b) shows the corresponding far-field cross sections of the intensity distributions with the second SPE of $\exp(-i\theta)$. Here the energy spreads out from the center to form an annular shape, as expected for a helical beam. However, for a hybrid beam, no spreading should occur, and there still is a central peak. These results clearly indicate that the emerging beam is indeed helical.

We also performed some experiments in which the laser operated with the fundamental TEM_{00} mode. This was achieved by replacing the SPE with a reflective mirror in the setup of Fig. 1, and adjusting the aperture. The measured output power was 0.9 W, which is significantly lower than 1.2 W obtained when the laser operated with the TEM_{01^*} helical mode. Thus, the advantage of intra-cavity mode shaping, rather than external mode shaping is twofold. First, the laser output power is higher since a larger volume of the gain medium is exploited. Secondly, there is no need for external beam shaping, which introduces both additional losses and some distortions to the output intensity distributions.

4. Concluding remarks

A method for obtaining pure helical laser beams was presented. These beams emerge directly from the laser, with controlled helicity, so they can be readily incorporated into a variety of applications.

Acknowledgements

This research was supported in part by Pamot Venture Capital Fund and the Israeli Ministry of Science.

References

[1] S.N. Khonina, V.V. Kotlyar, M.V. Shinkaryev, V.A. Soifer, G.V. Uspleniev, J. Mod. Opt. 39 (1992) 1147.
[2] J. Courtial, D.A. Robertson, K. Dholakia, L. Allen, M.J. Padgett, Phys. Rev. Lett. 81 (1998) 4828.
[3] H. He, M.E.J. Friese, N.R. Heckenberg, H. RubinszteinDunlop, Phys. Rev. Lett. 75 (1995) 826.
[4] S. Sato, Y. Harada, Y. Waseda, Opt. Lett. 19 (1994) 1807.
[5] T. Kuga, Y. Torii, N. Shiokawa, T. Hirano, Phys. Rev. Lett. 78 (1997) 4713.
[6] M.S. Soskin, V.N. Gorshkov, M.V. Vasnetsov, J.T. Malos, N.R. Heckenberg, Phys. Rev. A 56 (1997) 4064.
[7] T.R.M. Sales, G.M. Morris, OSA Annual Meeting, paper MR2, Portland, 1995.
[8] J.M. Vaughan, D.W. Willets, J. Opt. Soc. Am. 73 (1983) 1018.
[9] J. Arlt, K. Dholakia, L. Allen, M.J. Padgett, J. Mod. Opt. 45 (1998) 1231.
[10] M.W. Beijersbergen, L. Allen, H. Vanderveen, J.P. Woerdman, Opt. Commun. 96 (1993) 123.
[11] M.W. Beijersbergen, R.P.C. Coerwinkel, M. Kristiansen, J.P. Woerdman, Opt. Commun. 112 (1994) 321.
[12] E. Abramochkin, N. Losevsky, V. Volostnikov, Opt. Commun. 141 (1997) 59.
[13] V.E. Sherstobitov, A.Y. Rodionov, SPIE Proc. 3930 (2000) 62.
[14] M. Harris, C.A. Hill, J.M. Vaughan, Opt. Commun. 106 (1994) 161.
[15] R. Oron, Y. Danziger, N. Davidson, A.A. Friesem, E. Hasman, Opt. Commun. 169 (1999) 115.